THE JOURNAL OF PHYSICAL CHEMISTRY LETTERS
A JOURNAL OF THE AMERICAN CHEMICAL SOCIETY

Open Access
This article is licensed under CC-BY-NC-ND 4.0

pubs.acs.org/JPCL
Letter

A High-Density Supercritical Fluid of H_2

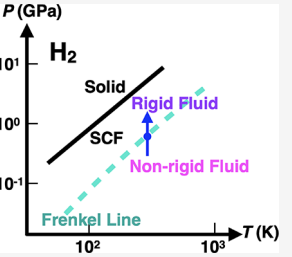
Atsuko Nakayama,* Naoto Fujii, Koji Hirama, Kentaro Hamada, Katsuya Shimizu, Yuki Nakamoto, Satoshi Nakano, Saori Kawaguchi-Imada, Yuichi Akahama, and Ayako Ohmura

Cite This: J. Phys. Chem. Lett. 2026, 17, 11754−11759

Read Online

ACCESS | Metrics & More | Article Recommendations | Supporting Information

ABSTRACT: This study aimed to elucidate the structural evolution of supercritical fluid hydrogen (SCF H_2) under high pressure. X-ray diffraction was performed on SCF H_2 using synchrotron radiation at room temperature. The structure factor $S(Q)$ was observed in a low-Q region at each pressure, revealing a crossover at around 0.56 GPa, consistent with our previous Raman spectroscopy results. The average volume per molecule was calculated at each pressure using the center-to-center distance between the nearest neighboring H_2 molecules, reflecting van der Waals interactions and compression of the internuclear distance. The volumes calculated from the face-centered cubic model were consistent with those derived from the cited equation of state, with a slight discrepancy that increased gradually with the pressure. This finding indicates that further densification following the crossover occurs primarily by intra-atomic/molecular mechanisms rather than intermolecular shortening of distances, which cannot be adequately explained by the close-packed coordination model alone.

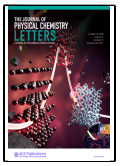


Many unresolved issues remain regarding the boundaries of the supercritical fluid (SCF) phase and its intrinsic physical properties. Numerous studies over the past 20 years have suggested that the SCF phase is not a simple single state but may consist of two states with different physical properties.[1] Initially, transition in dynamic properties such as the speed of sound and specific heat were proposed as an explanation for this.[2] However, subsequent research has reported that the SCF phase cannot be fully explained by the dualistic concept of static and dynamic properties alone.[3] In recent years, the concept of the 'Frenkel line' has been introduced, which classifies the SCF state into 'nonrigid liquid' and 'rigid liquid.[4,5] Various studies have confirmed that, for several pure substances, the Frenkel line acts as a boundary (or region) where the two states are separated by a smooth and wide-ranging crossover. For example, in SCF N_2, the intermolecular distance decreases with increasing pressure up to 150 MPa, resulting in an increase in the coordination number, which stabilizes at a pressure exceeding 150 MPa.[6] This compression is attributed to a direct reduction in the intermolecular N−N distance. Consequently, at temperatures and pressures exceeding the Frenkel line, for example, 300 K and 150 MPa, the aggregation state of N_2 molecules changes from nonrigid to rigid liquid-like behavior.

The SCF phase of H_2 has a density equivalent to that of liquid H_2 at 190 MPa and room temperature.[7] Furthermore, the transition from the SCF phase to solid phase I occurs at a pressure of 5.4 GPa and room temperature.[8,9] However, few studies have focused on the physical phenomena within an SCF. Until recently, H_2 was considered a homogeneous SCF phase at pressures up to 5.4 GPa and room temperature. In our previous study, we performed Raman spectroscopy on H_2 within the pressure range corresponding to the SCF phase at room temperature and systematically investigated the pressure dependence of the Raman shifts and line widths of the rotational and vibrational bands $S_0(J)$ and $Q_1(J)$, respectively.[10] As a result, we reported that a crossover occurs at 0.56 GPa at room temperature. According to the phase diagram of H_2, which includes the relationship between the temperatures and pressures at which the speed of sound is minimal,[2] we learned that the Frenkel line separating the SCF phase of H_2 passes through a pressure of approximately 0.56 GPa at room temperature.

Furthermore, in the postcrossover state of the SCF, pressure-induced changes in the relative intensities of rotons revealed that ortho−para conversion occurs at pressures of 1 GPa or higher, even in the absence of a catalyst.[10] Ortho−para conversion typically requires several days, even with a catalyst.[11] However, under pressure at room temperature, ortho−para conversion occurs within a few hours during Raman spectroscopy measurements. Elucidating the mechanism of ortho−para conversion induced by pressurization at room temperature without catalysts is crucial; however, research on this mechanism remains in its early stages. The intermolecular interactions increase with increasing pressure, affecting the nuclear interactions in the postcrossover state. To verify the mechanism underlying the ortho−para conversion observed in the higher-pressure SCF phase in the absence of catalysis, the collective state of H_2 molecules must be

Received: July 21, 2026
Revised: September 10, 2026
Accepted: September 11, 2026
Published: September 29, 2026



ACS Publications
© 2026 The Authors. Published by American Chemical Society

Downloaded from pubs.acs.org/jpclcd/article-pdf/17/41/11754/6870578/acs.jpclett.6c02439.pdf by NATL INST FOR MATLS SCIENCE (NIMS) user on 16 October 2026

investigated. Information on the structural changes in the SCF phase of H_2 could be key to examining the ortho-para conversion. To this end, H_2 must be replaced with D_2 to obtain structural information through neutron diffraction measurements. Nevertheless, neutron diffraction experiments on the SCF phase of D_2 using a diamond anvil cell (DAC) remain technically challenging. As an alternative to neutron diffraction, using X-ray diffraction (XRD) for structural analysis is worth testing. However, the scattering intensity of H_2 is extremely weak, so it remains to be seen how effective this approach will be. XRD experiments on the SCF phase of H_2 were attempted using synchrotron radiation (SR) at SPring-8[12] and yielded only three data points near 0.56 GPa, preventing a detailed characterization of the crossover. Furthermore, this analysis did not quantify the increase in the coordination number of the molecules, which indicates the growth of aggregates upon pressurization. Therefore, in this study, we performed XRD on H_2 using SR to obtain detailed data in the pressure range of up to 1.12 GPa at room temperature. We determined the structure factor at each pressure and investigated how the aggregation state of H_2 molecules changes in the SCF state.

To prepare the DAC, a phosphor bronze foil with an initial thickness of 300 μm was indented to 230 μm using diamond anvils (DAs) with culets of 800 μm in diameter. A 300 μm hole was drilled at the center of the indentation using an electrical discharge machine. A gasket was then placed on the lower DA. Ruby balls were placed on the upper DA as pressure markers to determine the magnitudes of the pressures applied to the samples. Normal H_2 gas with 99.99999% purity was compressed to 100 MPa using NIMS gas loading equipment[13] and then filled into the DAC at room temperature. The pressure in the DAC was determined from the fluorescence of the ruby R1-line using a pressure scale.[14]

The angle-dispersive method was used to obtain the diffraction patterns of the SCF phase using SR on beamline BL10XU at SPring-8. The X-ray was monochromatized to a wavelength λ = 0.4137(1) Å and introduced to the target through a pinhole collimator with a 40 μm diameter. Each XRD image was obtained by exposing the sample to X-rays for 120 s per run and averaging the intensity over ten runs. The average measurement temperature during the experiments was 299.4 K. All XRD data were collected on an imaging plate (IP) system (Rigaku R-AXIS IV++, readout resolution: 0.1 mm; active area: 300 × 300 mm^2). Two-dimensional XRD images, excluding the Kossel lines from the diamond and some spotty reflections that did not form diffraction rings, were integrated along the rings with a 0.01 degree of 2θ step. Each halo pattern was converted to an intensity vs 2θ profile using an IPanalyzer[15,16] and visualized using PDIndexer.[17] When using a DAC, H_2 diffraction and Compton scattering from the DAs were obtained simultaneously. Therefore, the XRD pattern of the empty DAC was measured and subtracted to remove the background diffraction (BG), yielding the diffraction pattern of H_2 at each pressure.

Strong Compton scattering from the DAs overlapped with the weak halo pattern of H_2, making it difficult to distinguish the true intensity of H_2 from the raw data. Figure 1a shows the X-ray scattering intensity of H_2 against the X-ray scattering vector $Q = 4\pi \sin\theta/\lambda$ measured at 1.17 GPa through the DAC. The scattering intensity obtained from the empty DAC was also plotted on the graph; however, in the regions around $Q \approx 3$ and 4.8 $Å^{-1}$, unknown diffraction peaks were observed even from the empty DAC. The scattered intensity after subtracting

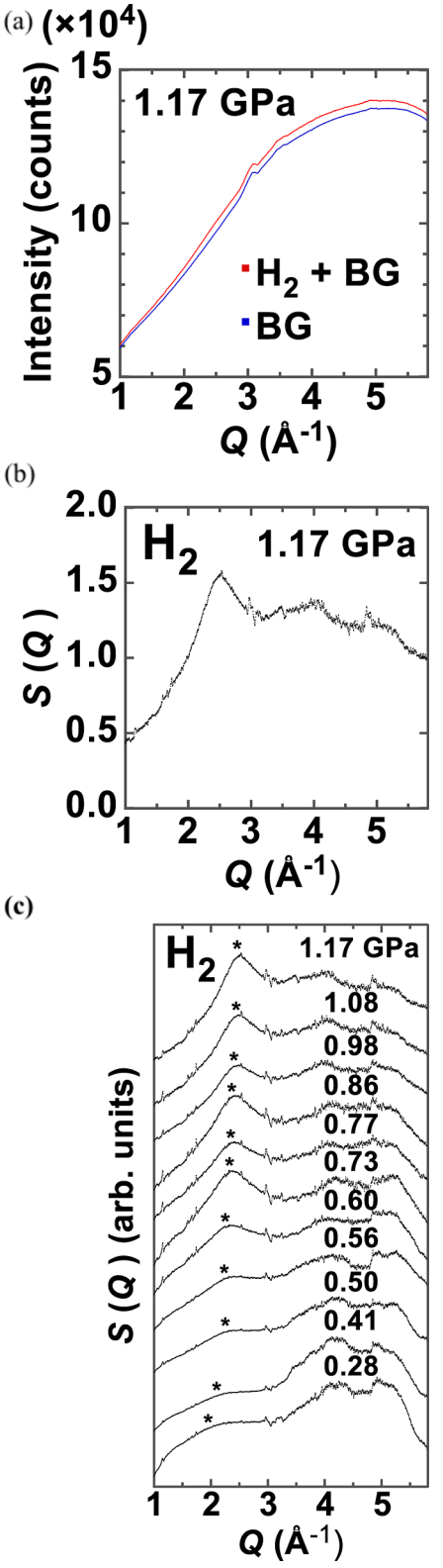


Figure 1. (a) X-ray scattering intensities from H_2 sealed within a diamond anvil cell (DAC) at 1.17 GPa and room temperature (H_2 + the background diffraction (BG), red dots) and an empty DAC (BG, blue dots). (b) Structure factor $S(Q)$ of H_2 at 1.17 GPa. The scattering intensity of H_2 alone was calculated by subtracting the BG intensity from that of H_2 + BG, as shown in Figure 1(a), and normalized using the intensity value at Q_{max} = 5.8 $Å^{-1}$ to obtain $S(Q)$. (c) Superimposed image of $S(Q)$ at each pressure. The peak

Downloaded from pubs.acs.org/jpclcd/article-pdf/17/41/11754/6870578/acs.jpclett.6c02439.pdf by NATL INST FOR MATLS SCIENCE (NIMS) user on 16 October 2026

https://doi.org/10.1021/acs.jpclett.6c02439
J. Phys. Chem. Lett. 2026, 17, 11754−11759

Figure 1. continued

intensities at approximately 2.5 $Å^{-1}$, marked by asterisks, increase with increasing pressure above 0.56 GPa, whereas the line width decreases.

the BG was obtained at each pressure and used to determine the Q_{max} value at each pressure. Minimizing the effects of ripple and measurement error required the use of the largest possible value of Q. Consequently, the value of Q_{max} was set to 5.8 $Å^{-1}$ for all pressures at which the scattering intensities were measured. All the scattering intensities were normalized using the intensities at Q_{max} = 5.8 $Å^{-1}$, resulting in the structure factors $S(Q)$, as shown in Figure 1b. Complete subtracting the BG from that of H_2, including that of the DAC, was unfeasible. Figure 1c shows a superimposed image of $S(Q)$ vs Q plots obtained at each pressure. Because the unremoved noise remained unchanged even under pressure, we concluded that it did not originate from the intrinsic diffraction of H_2 in the DAC. At a pressure above 0.41 GPa, a minimal increase in the baseline appeared at approximately $Q = 2 - 3$ $Å^{-1}$. However, when the pressure exceeded 0.56 GPa, a peak shape that is obscured in the BG, represented by asterisks, becomes determine the peak shape and grows as a main $S(Q)$ peak with increasing pressure. At the pressures above 0.56 GPa, the main $S(Q)$ peak shifts continuously and smoothly toward the high-Q side with increasing the pressure. The maximum intensity of the main $S(Q)$ peak, observed at $Q \approx 2.3$ $Å^{-1}$, exceeds $S(Q) = 1$ at pressures of 0.7 GPa. We identified that the mountain-shaped reflections and fine peaks, where the Q-values remain constant or jump discontinuously even when the pressure is varied, are not peaks from H_2, but rather noise from stray diamond crystal peaks. The SCF essentially consists of H_2 molecules arranged randomly, and the diffraction intensity comprises two contributions: scattering due to H−H bonds within the molecules and that due to correlations between H_2 molecules. The main $S(Q)$ peak observed here is located around 2.3−2.5 $Å^{-1}$, which has been identified as the intermolecular distance. Furthermore, considering from the results of high-pressure X-ray diffraction study on fluid H_2 at room temperature[12] and liquid H_2,[18] we identified the main $S(Q)$ peak obtained is the first $S(Q)$ peak for SCF H_2.

The main $S(Q)$ peak obtained at each pressure was analyzed using the Lorentzian function. Examples of analyses of $S(Q)$ vs Q plots obtained at pressures of 0.49, 0.56, and 1.17 GPa where these correspond to the pressure points before, during, and after the crossover, respectively (see Figure S1 in Supporting Information). Although the peak shapes were slightly broad and weak in the pressure range of 0.28−0.5 GPa, we managed to fit them using Lorentzian functions and obtain each parameter (see Table S1 in Supporting Information). Figure 2 shows the changes in the position and full width at half-maximum (FWHM) of the first $S(Q)$ peak with intensity $S(Q_{1st})$ with increasing pressure (see Table 2S in Supporting Information). As the pressure increased to 0.56 GPa, the peak position increases nearly linearly by 1.27 $Å^{-1}$/GPa. Following a temporary drop in the value of $S(Q_{1st})$ at 0.56 GPa, the peak position increases again at a rate of 0.37 $Å^{-1}$/GPa, which is lower than the value obtained below 0.56 GPa. The FWHM decreases with increasing the pressure, indicating a sharp decrease within the pressure range of approximately 0.5−0.6 GPa. At pressures exceeding 0.56 GPa, the rate of decrease in the FWHM gradually decreases. The pressure-induced narrowing of the FWHM for the XRD pattern observed in

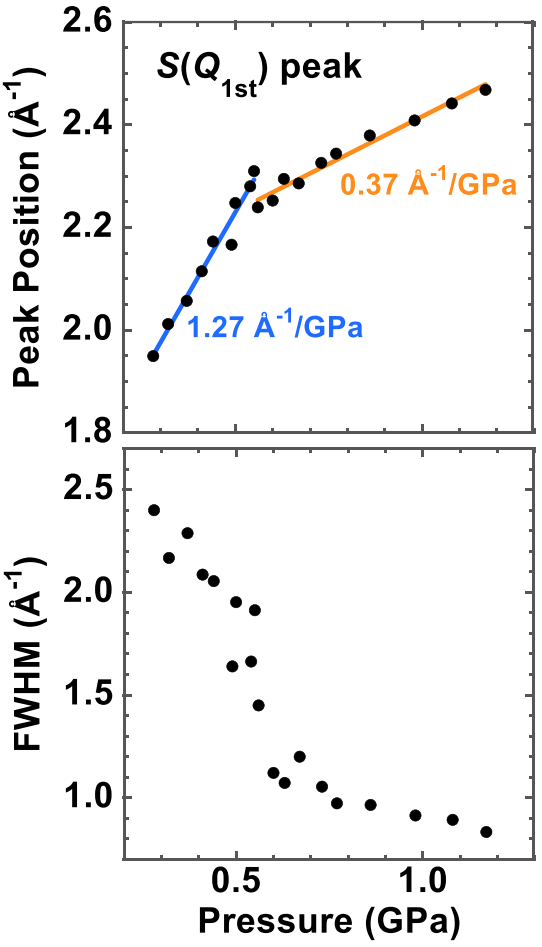


Figure 2. Pressure changes in the peak position (top) and full width at half-maximum (FWHM) (bottom) of the $S(Q_{1st})$ peak of supercritical fluid H_2. The errors associated with the values of peak positions and fwhm's obtained from the least-squares fit were smaller than the symbol size. At pressures below 0.56 GPa, the peak shift is 1.27 $Å^{-1}$/GPa; however, it decreases to 0.37 $Å^{-1}$/GPa above 0.56 GPa. The magnitude of the FWHM decreases significantly at approximately 0.5−0.6 GPa, and a gradual narrowing occurs.

SCF H_2 is explained as follows. In general, the larger the size of the ordered region, the narrower the width of the diffraction peak obtained owing to X-ray interference. As the pressure increases, the H_2 molecules within the fluids come closer together, and if the size of such larger molecular clusters increases, the structural units grow. Simultaneously, it is suggested that local molecular orientation correlations may increase, leading to a reduction in the disorder of the SCF phase and causing their states to change to more stable and ordered structures.

We estimated the volume per molecule of SCF H_2 to investigate the growth of the structural units under pressure. Initially, using a center position Q_{1st} of the $S(Q_{1st})$ peak, we obtained the average intermolecular distance of H_2, $d_{H_2-H_2} \approx 2\pi/Q_{1st}$, at each pressure, indicating the distance between the nearest hydrogen atoms of neighboring H_2 molecules, as illustrated in the inset in Figure 3. To calculate the molar volume, we needed the distance between the center of adjacent H_2 molecules $D_{H_2-H_2} \approx d_{H_2-H_2} + r_{H-H}$, where r_{H-H} is an internuclear distance of H_2. Therefore, we used our previous Raman spectral data[10] to calculate the values of r_{H-H} at each

Downloaded from pubs.acs.org/jpclcd/article-pdf/17/41/11754/6870578/acs.jpclett.6c02439.pdf by NATL INST FOR MATLS SCIENCE (NIMS) user on 16 October 2026

https://doi.org/10.1021/acs.jpclett.6c02439
J. Phys. Chem. Lett. 2026, 17, 11754−11759

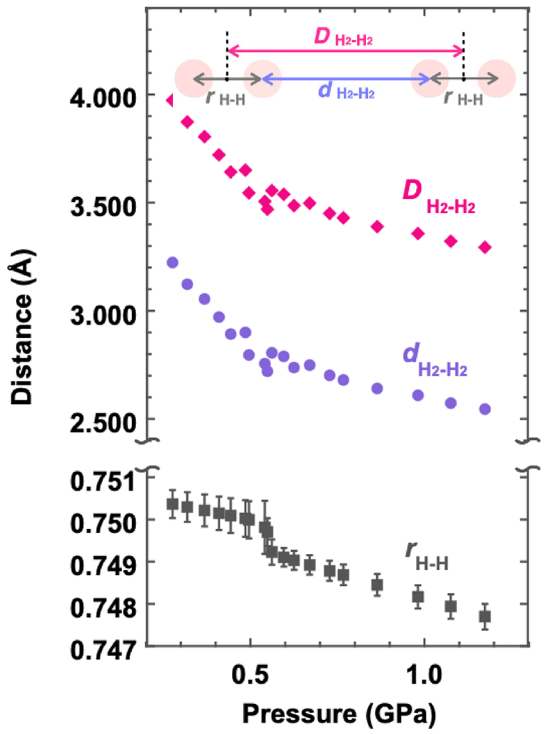


Figure 3. Pressure dependence of distances $D_{H_2-H_2}$, $d_{H_2-H_2}$, and r_{H-H}. The pink solid rhombuses, lavender solid circles, and black solid squares represent distances $D_{H_2-H_2}$, $d_{H_2-H_2}$, and r_{H-H} at varying pressures, respectively. The magnitudes of error bars for data labeled $D_{H_2-H_2}$ and $d_{H_2-H_2}$ are smaller than the respective symbols. The inset schematic shows the relative positions of $D_{H_2-H_2}$, $d_{H_2-H_2}$, and r_{H-H}.

pressure. If we consider only the normal vibration level ($\nu = 0$), the rotational energy level $E(J)$ can be expressed as follows:[19]

$$E(J) = B_0 J(J+1) - D_0 J^2 (J+1)^2 + \ldots \quad (1)$$

where the first term represents the J dependence of the rotational energy of a rigid rotor, whereas the coefficients $B_0$and D_0 account for the rotational constants; only the first two terms in eq 1 are considered. The internuclear distance r_{H-H} can be derived using $B_0 = \frac{h}{8\pi^2 c\mu}\langle r_{H-H}{}^2\rangle_0$ where h is Planck's constant, c is the speed of light, μ is the reduced mass of the molecule, and the symbol $\langle\cdots\rangle_0$ denotes averaging over the zero-point motion of the $\nu = 0$ normal vibration level. The rotational transition energy, $S_0(J)$ can be obtained using eq (1), as follows:

$$S_0(J) = E(J+2) - E(J) = (4B_0 - 6D_0)\left(J + \frac{3}{2}\right) - 8D_0\left(J + \frac{3}{2}\right)^3 \quad (2)$$

The constants B_0 and D_0 were obtained using eq (2) via least-squares fitting using the three rotational vibrational levels $S_0(J)$ (J 0, 1, 2), as observed in the Raman spectra at each pressure. We then calculated the value of $r_{H-H} = \langle r_{H-H}{}^2\rangle^{1/2}$, which represents the experimentally derived internuclear distance of the H_2 molecules.

Figure 3 shows the pressure dependence of $d_{H_2-H_2}$, r_{H-H}, and $D_{H_2-H_2}$. The distance $d_{H_2-H_2}$ decreased as the pressure increased up to 0.56 GPa, exhibiting a jump in the data at approximately 0.56 GPa. When the pressure exceeded 0.56 GPa, the value of $d_{H_2-H_2}$ decreased again; however, the contraction rate was smaller than that observed at pressures below 0.56 GPa. Conversely, the r_{H-H} distance exhibited an increase in the contraction rate at pressure exceeding 0.56 GPa, indicating that the space between H_2 molecules as well as the molecules themselves were compressed. This finding suggests that the intermolecular repulsive forces increased in the post crossover state in the SCF, resulting in a reduction in the space between the H_2 molecules and compression of the H_2 molecules. The pressure-induced changes in $d_{H_2-H_2}$, r_{H-H}, and $D_{H_2-H_2}$ provided evidence that H_2 underwent the crossover at 0.56 GPa. At this point, the pressure-dependent Raman line width exhibited a remarkable shift, indicating changes in the relaxation mechanism of the rotational and vibrational modes.[10] This finding supports the conclusion that the collective state of H_2 molecules changes, resulting in local high-density states.

The crossover observed in the SCF phases for neon,[4] N_2,[6] and methane[20] occur along their respective Frenkel lines. It has been observed that, in the pressure range exceeding each Frenkel line, the coordination number of molecules gradually increases with increasing the pressure. The sharp change with increasing the pressure observed at around 0.56 GPa for H_2 is thought to indicate that the crossover has occurred across the Frenkel line. In the pressure range beyond the Frenkel line, H_2 is also expected to exhibit an increase in the coordination number of its molecule.

Subsequently, an average volume per molecule was calculated using the values of $D_{H_2-H_2}$ obtained at 0.56 GPa and above to investigate an appropriate model explaining the pressure change in volume following the crossover in SCF phase. In this model, H_2 molecules were assumed to be hard spheres, and to take account of the molecules' coordination number, it was speculated that the molecules are ideally packed in to cubic lattices. When the molecules are arranged in a simple-cubic (SC) coordination model with a lattice parameter $a = D_{H_2-H_2}$, the average volume per molecule is calculated as $V_{SC} = a^3 = D_{H_2-H_2}{}^3$. In a body-centered cubic (BCC) coordination model, the relationship between $D_{H_2-H_2}$ and the lattice parameter a is given by $a = \frac{2}{\sqrt{3}}D_{H_2-H_2}$, and the average volume per molecule, V_{BBC}, is obtained as $V_{BCC} = \frac{a^3}{2} = \frac{4}{3\sqrt{3}}(D_{H_2-H_2})^3 \approx 0.7698(D_{H_2-H_2})^3$. A coordination model of a face-centered cubic (FCC) lattice has a close-packed structure with a coordination number of 12. The average volume per molecule, V_{FCC}, is calculated as $V_{FCC} = \frac{a^3}{4} = \frac{\sqrt{2}^3}{4}(D_{H_2-H_2})^3 \approx 0.7071(D_{H_2-H_2})^3$, using the relation $a = \sqrt{2}(D_{H_2-H_2})$. Figure 4 shows the pressure changes in the average volumes per H_2 molecule, assuming that the postcrossover state in the SCF phase exhibits a short-range order with SC, BCC, or FCC coordination of H_2 molecules. For comparison, we referred to the average volume per molecule calculated at an experimental temperature of 299.4 K for XRD using the equation of state (EOS) for the H_2 SCF phase, as derived by Mills et al.[21] They measured the molar volume using a piston−cylinder apparatus and defined the EOS for fluid n-H_2 based on their detailed experimental results. No abrupt volume changes or transitions were observed at any

Downloaded from pubs.acs.org/jpclcd/article-pdf/17/41/11754/6870578/acs.jpclett.6c02439.pdf by NATL INST FOR MATLS SCIENCE (NIMS) user on 16 October 2026

https://doi.org/10.1021/acs.jpclett.6c02439
J. Phys. Chem. Lett. 2026, 17, 11754−11759

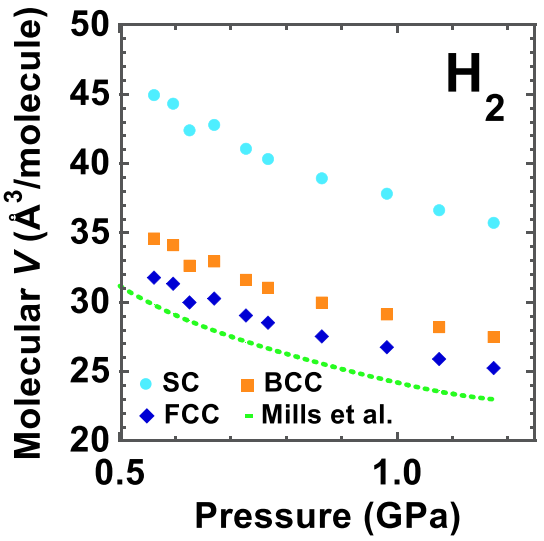


Figure 4. Pressure changes in the average volume per H_2 molecule, assuming that the postcrossover state exhibits a short-range order with SC, BCC, or FCC coordination of H_2 molecules. The light-blue solid circles, orange solid squares, and blue solid rhombuses represent the volumes at pressures obtained by applying $D_{H_2-H_2}$ data to the SC, BCC, and FCC coordination models, respectively. The green curve represents the average volume per molecule calculated at an experimental temperature of 299.4 K for XRD using the EOS for the H_2 SCF phase, as derived by Mills et al.[21]

reported pressure. Therefore, we did not refer to the crossover here; instead, we compared only the volume per molecule based on the molecular coordination model with the EOS results. For instance, the volume at 9.8 kbar (≈ 0.98 GPa) was approximately 24.4 $Å^3$ per molecule using EOS. However, using the value of $D_{H_2-H_2}$ at 0.98 GPa, the volume per molecule calculated using the SC, BCC, and FCC coordination models was 37.84, 29.13, and 26.75 $Å^3$, respectively. The volume derived from the FCC coordination model was closer to the volume obtained by EOS, with a minimal difference of approximately 2.35 $Å^3$. As the center-to-center distance between the H_2 molecules has been corrected based on their dumbbell-shaped molecular structure, our data provide microscopic insights into the shape of H_2 molecules and the intermolecular gaps formed by short-range order. Mills' data characterized the macroscopic result of the number of H_2 molecules contracted as a whole by deforming their electron clouds under high pressure. The increase in the contraction of r_{H-H} following the crossover, as shown in Figure 3, suggests the acceleration of the compression of the electron cloud of H_2 molecules in the postcrossover state.

It is known that the solid-phase I of H_2 exhibits a hexagonal close-packed (hcp) structure with a coordination number of 12.[22] Following the SCF phase, the solid phase I also exhibits a coordination number of 12; but, the solid phase I possesses a characteristic stacking structure, and the hcp structure should be distinguished from the FCC structure. On the other hand, an analysis of the coordination number based on the nearest-neighbor distance and molecular volume does not allow us to distinguish between the FCC and hcp coordination models. Therefore, from here, we refer to it as "FCC/hcp-like coordination model". Although the coordination number can be 12 following the crossover, the number is fundamentally dependent on the FCC/hcp-like coordination model. On the other hand, this suggests that it may be a general characteristic for diatomic molecular fluids to change in the FCC/hcp-like coordination once crossing the Frenkel line. The increase in the coordination number has been found in SCF N_2 reaching the coordination number of 12 over various ranges of pressure and temperature.[23] At pressures of 0.98 GPa and above, the volume difference increased slightly, indicating that the FCC/hcp-like model could not fully explain this phenomenon. For instance, in the Ni−P alloy, the maximum packing fraction for the random packing of hard spheres was 0.64, whereas for soft spheres, the packing fraction exceeded 0.67.[24] Therefore, when pressure was applied from the outside, the particles were compressed and deformed, increasing the contact area and number of contacts between the particles and reducing the gaps between them. For H_2, an increase in the ratio of the decrease in the internuclear distance was observed following the crossover. As shown in Figure 4, the packing fraction is expected to be slightly higher than that of FCC/hcp-like coordination model. This finding may also demonstrate the potential limitations of explaining the SCFs of H_2 molecules using a hard-sphere model.

Regarding H_2, it was not possible to determine the two-body distribution function with sufficient accuracy due to insufficient diffraction intensity of $S(Q)$. Consequently, reliable coordination numbers[25] could not be obtained, and it was not possible to find the detailed pressure dependence of the coordination numbers as reported for N_2.[6] On the other hand, although the approach taken in this study differs from conventional methods, as estimation of the volume pre H_2 molecule based on the mean intermolecular distances obtained suggests that the system forms a state of equal or denser density——equivalent to or greater than the FCC structure——than that indicated by the conventional SCF-phase equation of state.

In summary, we determined the structure factor of H_2 at each pressure following the crossover in the SCF phase. The results revealed that the crossover occurs at 0.56 GPa. Assuming the FCC coordination of H_2 model, the average volume per molecule and the coordination number following the crossover were calculated using the center-to-center distance between the nearest-neighbor molecules determined experimentally. This model indicates that the rigid fluid forms under conditions that exceed the Frenkel line.

■ ASSOCIATED CONTENT

Supporting Information

The Supporting Information is available free of charge at https://pubs.acs.org/doi/10.1021/acs.jpclett.6c02439.

Additional analysis of the $S(Q)$ versus Q plots, results of peak fitting using Lorentzian and Gaussian functions, parameters of peaks 0−6 determined by peak analysis using Lorentzian and Gaussian functions, and parameters of the main and unknown peaks determined by peak analysis using Lorentzian functions at all the pressure points measured. (DOCX)

■ AUTHOR INFORMATION

Corresponding Author

Atsuko Nakayama − *Department of Mathematical Science and Physics, Faculty of Science and Engineering, Iwate University, Morioka, Iwate 020-8551, Japan;* orcid.org/0009-0002-0016-3750; Email: atsuko@iwate-u.ac.jp

https://doi.org/10.1021/acs.jpclett.6c02439
J. Phys. Chem. Lett. 2026, 17, 11754−11759

Downloaded from pubs.acs.org/jpclcd/article-pdf/17/41/11754/6870578/acs.jpclett.6c02439.pdf by NATL INST FOR MATLS SCIENCE (NIMS) user on 16 October 2026

Authors

Naoto Fujii − *Graduate School of Arts and Science, Iwate University, Morioka, Iwate 020-8551, Japan*
Koji Hirama − *Graduate School of Arts and Science, Iwate University, Morioka, Iwate 020-8551, Japan*
Kentaro Hamada − *Graduate School of Arts and Science, Iwate University, Morioka, Iwate 020-8551, Japan*
Katsuya Shimizu − *KYOKUGEN, Center for Science and Technology under Extreme Conditions, The University of Osaka, Toyonaka, Osaka 560-8531, Japan; Geodynamics Research Center, Ehime University, Matsuyama, Ehime 790-8577, Japan;* orcid.org/0000-0003-0560-8325
Yuki Nakamoto − *KYOKUGEN, Center for Science and Technology under Extreme Conditions, The University of Osaka, Toyonaka, Osaka 560-8531, Japan*
Satoshi Nakano − *National Institute for Materials Science (NIMS), Tsukuba, Ibaraki 305-0044, Japan;* orcid.org/0000-0002-7010-9867
Saori Kawaguchi-Imada − *Diffraction and Scattering Division, Japan Synchrotron Radiation Research Institute, Hyogo 679-5198, Japan; Office of Institutional Advancement and Communications, Kyoto University, Hyogo 679-5198, Japan*
Yuichi Akahama − *Graduate School of Material Science, University of Hyogo, Hyogo 678-1297, Japan;* orcid.org/0000-0003-2736-9855
Ayako Ohmura − *Faculty of Science, Niigata University, Niigata 950-2181, Japan*

Complete contact information is available at: https://pubs.acs.org/10.1021/acs.jpclett.6c02439

Notes

The authors declare no competing financial interest.

■ ACKNOWLEDGMENTS

This study was supported by JSPS KAKENHI (grant number JP1A24K014270) and partly supported by the NIMS Cooperative Research Promotion Program from the National Institute for Materials Science Cooperative Promotion). Synchrotron radiation experiments were performed at BL10XU of SPring-8 with the approval of the Japanese Synchrotron Radiation Research Institute (Proposal No. [2024B1268]).

■ REFERENCES

(1) Gorelli, F. A.; Santoro, M.; Scopigno, T.; Krisch, M.; Bryk, T.; Ruocco, G.; Ballerini, R. Inelastic x-ray scattering from high pressure fluids in a diamond anvil cell. *Appl. Phys. Lett.* **2009**, *94* (7), No. 074102.
(2) Trachenko, K.; Brazhkin, V. V.; Bolmatov, D. Dynamic transition of supercritical hydrogen: defining the boundary between interior and atmosphere in gas giants. *Phys. Rev. E* **2014**, *89* (3), No. 032126.
(3) Bryk, T. Comment on "Dynamic transition of supercritical hydrogen: defining the boundary between interior and atmosphere in gas giants". *Phys. Rev. E* **2015**, *91* (3), No. 036101.
(4) Prescher, C.; Fomin, Y. D.; Prakapenka, V. B.; Stefanski, J.; Trachenko, K.; Brazhkin, V. V. Experimental evidence of the Frenkel line in supercritical neon. *Phys. Rev. B* **2017**, *95* (13), No. 134114.
(5) Bryk, T.; Gorelli, F. A.; Mryglod, I.; Ruocco, G.; Santoro, M.; Scopigno, T. Behavior of supercritical fluids across the "Frenkel line". *J. Phys. Chem. Lett.* **2017**, *8* (20), 4995−5001.
(6) Proctor, J. E.; Pruteanu, C. G.; Morrison, I.; Crowe, I. F.; Loveday, J. S. Transition from gas-like to liquid-like behavior in supercritical N_2. *J. Phys. Chem. Lett.* **2019**, *10* (21), 6584−6589.
(7) Mills, R. L.; Liebenberg, D. H.; Bronson, J. C.; Schmidt, L. C. Procedure for loading diamond cells with high-pressure gas. *Rev. Sci. Instrum.* **1980**, *51* (7), 891−895.
(8) Mao, H. K.; Bell, P. M. Observations of hydrogen at room temperature (25 °C) and high pressure (to 500 kilobars). *Science* **1979**, *203* (4384), 1004−1006.
(9) Diatschenko, V.; Chu, C. W.; Liebenberg, D. H.; Young, D. A.; Ross, M.; Mills, R. L. Melting curves of molecular hydrogen and molecular deuterium under high pressures between 20 and 373 K. *Phys. Rev. B* **1985**, *32* (1), 381−389.
(10) Nakayama, A.; Isurugi, Y.; Serizawa, Y.; Nakano, S.; Ohmura, A.; Ishikawa, F. Phase transition in fluid hydrogen at room temperature. *J. Phys. Soc. Jpn.* **2022**, *91* (9), No. 093601.
(11) Abe, H.; Mizoguchi, H.; Eguchi, R.; Hosono, H. Exploration of heterogeneous catalyst for molecular hydrogen ortho-para conversion. *Exploration* **2024**, *4* (3), No. 20230040.
(12) Akahama, Y.; Miyamoto, R.; Nakano, S.; Kawaguchi, S.; Hirao, N.; Ohishi, Y. High-pressure Raman scattering and x-ray diffraction studies of the supercritical fluid of hydrogen. *J. Appl. Phys.* **2020**, *128* (13), No. 135901.
(13) Kenichi, T.; Sahu, P. C.; Yoshiyasu, K.; Yasuo, T. Versatile gas-loading system for diamond-anvil cells. *Rev. Sci. Instrum.* **2001**, *72* (10), 3873−3876.
(14) Zha, C. S.; Mao, H. K.; Hemley, R. J. Elasticity of MgO and a primary pressure scale to 55 GPa. *Proc. Natl. Acad. Sci. U.S.A.* **2000**, *97* (25), 13494−13499.
(15) Seto, Y.; Nishio-Hamane, D.; Nagai, T.; Sata, N. Development of a software suite on X-ray diffraction experiments. *Review of High Pressure Science and Technology* **2010**, *20* (3), 269−276.
(16) https://github.com/seto77/IPanalyzer/, Date accessed: 10 December 2024.
(17) https://github.com/seto77/PDIndexer/ (accessed Date accessed: 10 December 2024).
(18) Weck, G.; Garbarino, G.; Loubeyre, P.; Datchi, F.; Plisson, T.; Mezouar, M. Liquid hydrogen structure factor to 5 GPa and evidence of a crossover between two density evolutions. *Phys. Rev. B* **2015**, *91*, No. 180204(R).
(19) Ulivi, L.; Zoppi, M.; Gioè, L.; Pratesi, G. Molecular hydrogen internuclear distance in high-pressure fluid and solid phases at room temperature. *Phys. Rev. B* **1998**, *58* (5), 2383−2386.
(20) Smith, D.; Hakeem, M. A.; Parisiades, P.; Maynard-Casely, H. E.; Foster, D.; Eden, D.; Bull, D. J.; Marshall, A. R. L.; Adawi, A. M.; Howie, R.; Sapelkin, A.; Brazhkin, V. V.; Proctor, J. E. Crossover between liquidlike and gaslike behavior in CH_4 at 400 K. *Phys. Rev. E* **2017**, *96* (5−1), No. 052113.
(21) Mills, R. L.; Liebenberg, D. H.; Bronson, J. C. Equation of state of fluid n−H_2 from P−V−T and sound velocity measurements to 20 kbar. *J. Chem. Phys.* **1977**, *66*, 3076−3084.
(22) Hazen, R. M.; Mao, H. K.; Finger, L. W.; Hemley, R. J. Single-crystal x-ray diffraction of n-H_2 at high pressure. *Phys. Rev. B* **1987**, *36* (7), 3944−3947.
(23) Pruteanu, C. G.; Daramola, A. D.; Kirsz, M.; Robertson, C. E. A.; Jonse, L. L.; Wang, T.; Loveday, J. S.; Ackland, G. J.; Alderman, O. L. G.; Proctor, J. E. Subcritical Determination of Frenkel Line in Liquid Nitrogen, the Emergent Final Picture, and a Universal Equation for the Coordination Number of real Fluids. *J. Phys. Chem. B* **2025**, *129*, 3420−3427.
(24) Connell, G. A. N. Dense random packings of hard and compressible spheres. *Solid State Commun.* **1975**, *16* (1), 109−112.
(25) Eggert, J. H.; Weck, G.; Loubeyre, P.; Mezouar, M. Quantitative structure factor and density measurements of high-pressure fluids in diamond anvil cells by x-ray diffraction: Argon and water. *Phys. Rev. B* **2002**, *65* (17), No. 174105.

Downloaded from pubs.acs.org/jpclcd/article-pdf/17/41/11754/6870578/acs.jpclett.6c02439.pdf by NATL INST FOR MATLS SCIENCE (NIMS) user on 16 October 2026